

Breather-to-soliton transitions and nonlinear wave interactions for higher-order generalized Gerdjikov-Ivanov equation

Yanan Wang(王亚男) and Minghe Zhang(张明赫)
Citation: Chin. Phys. B, 2026, 35 (**8**): 080202. DOI: 10.1088/1674-1056/ae15f2
http://cpb.iphy.ac.cn; http://iopscience.iop.org/cpb

What follows is a list of articles you may be interested in

Degenerate solitons and asymptotic analysis for a three-coupled fourth-order nonlinear Schrödinger system in an alpha helical protein

Dan-Yu Yang(杨丹玉)
Chin. Phys. B, 2026, 35 (**2**): 020201. DOI: 10.1088/1674-1056/adf4a5

An *N*-breather solution and hybrid solutions of rogue wave and breather for complex mKdV equation

Wenjing Hu(胡文静) and Hasi Gegen(葛根哈斯)
Chin. Phys. B, 2025, 34 (**7**): 070202. DOI: 10.1088/1674-1056/adcdef

Asymptotic analysis on bright solitons and breather solutions of a generalized higher-order nonlinear Schrödinger equation in an optical fiber or a planar waveguide

Xin Zhao(赵鑫), Zhong Du(杜仲), Li-Jian Zhou(周立俭), Rong-Xiang Liu(刘荣香), and Xu-Hu Wang(王绪虎)
Chin. Phys. B, 2024, 33 (**11**): 110204. DOI: 10.1088/1674-1056/ad7e9e

Diverse soliton solutions and dynamical analysis of the discrete coupled mKdV equation with 4×4 Lax pair

Xue-Ke Liu(刘雪珂) and Xiao-Yong Wen(闻小永)
Chin. Phys. B, 2023, 32 (**12**): 120203. DOI: 10.1088/1674-1056/acf122

Resonant interactions among two-dimensional nonlinear localized waves and lump molecules for the (2+1)-dimensional elliptic Toda equation

Fuzhong Pang(庞福忠), Hasi Gegen(葛根哈斯), and Xuemei Zhao(赵雪梅)
Chin. Phys. B, 2023, 32 (**5**): 050205. DOI: 10.1088/1674-1056/acb2c2

Breather-to-soliton transitions and nonlinear wave interactions for higher-order generalized Gerdjikov–Ivanov equation

Yanan Wang(王亚男)[1] and Minghe Zhang(张明赫)[2,†]

[1] *School of Mathematical Science, Beihang University, Beijing* 102206, *China*
[2] *School of Mathematical Science, Harbin Engineering University, Harbin* 150001, *China*

(Received 15 August 2025; revised manuscript received 9 October 2025; accepted manuscript online 22 October 2025)

We systematically investigate the intricate dynamics of the breather-to-soliton transitions and nonlinear wave interactions for the higher-order generalized Gerdjikov–Ivanov equation. The transition conditions of the breather-to-soliton are established and the novel nonlinear converted waves, including the W-shaped soliton, multi-peak soliton, anti-dark soliton and periodic wave solution are discussed. Meanwhile, the interactions among the above nonlinear converted waves are explored by choosing appropriate parameters. Furthermore, we derive the double-pole solutions exhibiting breather-to-soliton transitions and employ the asymptotic analysis method to analyze the dynamics of the asymptotic solitons for the double-pole anti-dark soliton. This work deepens the fundamental understanding of nonlinear wave metamorphosis induced by higher-order terms in integrable systems.

Keywords: higher-order generalized Gerdjikov–Ivanov equation, breather-to-soliton transitions, double-pole converted waves, asymptotic analysis

PACS: 02.30.Ik, 02.30.Jr, 05.45.Yv

DOI: 10.1088/1674-1056/ae15f2 **CSTR:** 32038.14.CPB.ae15f2

1. Introduction

It is well known that solitons, breathers, and rogue waves represent fundamental nonlinear wave phenomena, each exhibiting distinct dynamic behaviors across diverse physical domains. They have attracted extensive attention due to their emergence in numerous nonlinear models involving various fields such as plasma physics, nonlinear optics, hydrodynamics, and Bose–Einstein condensations (BEC).[1–6]

Recently, the state transition mechanisms between the breathers (or rogue waves) and solitons have been explored in various nonlinear models. Breathers and rogue waves can turn into solitons through the Raman effect. This idea is backed up by evidence in Refs. [7,8]. Similar to the effect of trapping perturbation on soliton trajectories and the influence of Rabi coupling on soliton-type conversion in BEC,[9–11] the higher-order term induces the transition of breathers to show structural diversity by regulating the balance between dispersion and nonlinearity.

A wealth of converted wave forms have been derived from breathers and rogue waves under appropriate transition conditions. The first case involves the nonlinear models featuring higher-order terms that contribute to the state transitions.[12] The mixed nonlinear Schrödinger equation (NLS),[13] fifth-order NLS,[14] higher-order generalized NLS,[15] and six-order NLS equation[16] have been successively discovered to possess various converted waves. The Hirota equation[17–19] also exhibits the breather-to-soliton transition phenomenon. Meanwhile, Sasa–Satsuma equation[20] and the high-order Chen–Lee–Liu equation have also been considered.[21] Another case occurs in coupled equations describing multi-field interactions which facilitate the state transitions. The transitions of the breather solution have been progressively discussed in the coupled NLS equation,[22] coupled Hirota equation,[23,24] multi-component AB system,[25–27] coupled Fokas–Lenells system,[28] and coupled extended modified Korteweg–de Vries system.[29]

In addition, multi-pole solitons, also known as degenerate solitons, have attracted extensive attention in the academic research.[30–32] They can describe the interactions among multiple chirped pulses with the same amplitude in the optical fibers and in the quantum physical field. Hence, the double-pole breather-to-soliton represents a significant area of research.

In this article, we focus on the the higher-order generalized Gerdjikov–Ivanov equation (HGGI),

$$\begin{aligned} &\mathrm{i}q_t + 2\mathrm{i}q_{xxx} + \left[(16\delta+4)|q|^2 - 4\delta\right]q_{xx} + (4\delta+1)q^2q_{xx}^* + (12\delta+3)q^{*2}q_x^2 \\ &+ \left[(20\delta+2)qq_x^* - \left(48\delta^2+30\delta+\frac{15}{4}\right)\mathrm{i}|q|^4 + \left(24\delta^2+6\delta\right)\mathrm{i}|q|^2 - 2\mathrm{i}\delta^2\right]q_x \end{aligned}$$

†Corresponding author. E-mail: zhangminghe@hrbeu.edu.cn

© 2026 Chinese Physical Society and IOP Publishing Ltd. All rights, including for text and data mining, AI training, and similar technologies, are reserved.

$$-\left[(24\delta^2+6\delta)|q|^2q^2-8\delta^2q^2\right]\mathrm{i}q_x^*-\left(16\delta^3+24\delta^2+\frac{15}{2}\delta+\frac{5}{8}\right)|q|^6q$$
$$+\left(16\delta^3+12\delta^2+\frac{3}{2}\delta\right)|q|^4q-\left(4\delta^3+\delta^2\right)|q|^2q+2\delta^3q=0, \tag{1}$$

where δ is an arbitrary real number. It exerts a significant influence on the self-steepening effect during transmission, which corresponds to the self-frequency shift in Raman scattering. Guan, Yang, Meng, and Liu obtained the higher-order rogue wave solutions and their dynamic properties for the HGGI equation by generalized Darboux transformation (DT).[33] The soliton, breather and new rogue wave solutions of the HGGI equation were reached by Zhao, Wang and Yang through DT method.[34] The multi-positon solutions, interaction solutions and the modulation instability for the HGGI equation were exhibited by Zhao, Wang and Zhang.[35]

This paper is organized as follows: In Section 2, we provide the state transition conditions and obtain different nonlinear converted waves including W-shaped soliton, anti-dark soliton, multi-peak soliton and periodic waves. In Section 3, the interactions between the above various nonlinear converted waves are investigated. In Section 4, double-pole converted waves are derived and the asymptotic analysis is given for the double-pole anti-dark soliton to obtain the explicit expression of the asymptotic solitons.

2. Breather-to-soliton transitions

In this section, we discuss the existence conditions for several types of nonlinear converted waves by analyzing the explicit expression of the first-order solution on the plane wave background. The Lax pair for Eq. (1) have given in Ref. [35] as follows:

$$\Phi_x=P\Phi,\quad \Phi_t=Q\Phi, \tag{2}$$

where $\Phi=(\psi,\phi)^{\mathrm{T}}$ is the complex vector function and

$$P=\begin{pmatrix}\frac{1}{2}\mathrm{i}\lambda^2+\mathrm{i}\delta|q|^2 & \frac{1}{2}\lambda q\\ -\frac{1}{2}\lambda q^* & -\frac{1}{2}\mathrm{i}\lambda^2-\mathrm{i}\delta|q|^2\end{pmatrix},$$
$$Q=\begin{pmatrix}Q_1 & Q_2\\ Q_3 & -Q_1\end{pmatrix},$$

with

$$Q_1=\frac{1}{2}\mathrm{i}q^*q_{xx}+\frac{1}{2}\mathrm{i}qq_{xx}^*+\frac{1}{16}\left[-8\mathrm{i}q_x^*+(48\delta+12)|q|^2q-\left(8\lambda^2+16\delta\right)q^*\right]q_x-3\left[q^*\left(\delta+\frac{1}{4}\right)q-\frac{\lambda^2}{6}-\frac{\delta}{3}\right]qq_x^*$$
$$-6\mathrm{i}|q|^6\left(\delta^2+\frac{\delta}{2}+\frac{5}{96}\right)+4\mathrm{i}\left(\delta+\frac{3}{16}\right)\left(\frac{\lambda^2}{2}+\delta\right)|q|^4-\frac{\mathrm{i}\left(\lambda^2+\delta\right)^2|q|^2}{2}+\mathrm{i}\lambda^6+2\mathrm{i}\lambda^4\delta+\mathrm{i}\lambda^2\delta^2+\mathrm{i}\delta^3,$$
$$Q_2=2\lambda\left[-\frac{q_{xx}}{2}+\left[3\mathrm{i}\left(\delta+\frac{1}{4}\right)|q|^2-\frac{1}{2}\mathrm{i}\lambda^2-\mathrm{i}\delta\right]q_x+\left[\mathrm{i}\delta qq_x^*+\frac{(\lambda^2+\delta)^2}{2}-2\left(\delta+\frac{1}{4}\right)\left(\frac{\lambda^2}{2}+\delta\right)|q|^2\right.\right.$$
$$\left.\left.+2\left(\delta^2+\frac{3}{4}\delta+\frac{3}{32}\right)|q|^4\right]q\right],$$
$$Q_3=2\lambda\left[\frac{q_{xx}^*}{2}+\left[3\mathrm{i}\left(\delta+\frac{1}{4}\right)|q|^2-\frac{1}{2}\mathrm{i}\lambda^2-\mathrm{i}\delta\right]q_x^*+\left[\mathrm{i}\delta^*qq_x-\frac{(\lambda^2+\delta)^2}{2}+2\left(\delta+\frac{1}{4}\right)\left(\frac{\lambda^2}{2}+\delta\right)|q|^2\right.\right.$$
$$\left.\left.-2\left(\delta^2+\frac{3}{4}\delta+\frac{3}{32}\right)|q|^4\right]q^*\right],$$

where λ is the complex spectral parameter and the zero curvature equation $P_t-Q_x+PQ-QP=0$ generates original Eq. (1).

We introduce the seed solution $q[0]=d\,\mathrm{e}^{\mathrm{i}(ax+bt)}$ to Eq. (2) with

$$b=-16\delta^3d^6-24\delta^2d^6-\frac{15}{2}d^6\delta-\frac{5}{8}d^6+16\delta^3d^4+24\delta^2d^4a+12\delta^2d^4+24d^4\delta a+\frac{3}{2}d^4\delta+\frac{15}{4}d^4a-4\delta^3d^2$$
$$-16\delta^2d^2a-\delta^2d^2-12d^2a^2\delta-6d^2\delta a-6d^2a^2+2a^3+4a^2\delta+2\delta^2a+2\delta^3.$$

Based on the above expression, it is found the parameter δ affects the dispersion relation of the equation. According to the DT given in Ref. [34], we assume $\Phi_j=(\psi_j,\phi_j)^{\mathrm{T}}$, $j=1,\ldots,n$ are the eigenfunctions under $\lambda=\lambda_j$, $j=1,\ldots,n$, then we can obtain the n-order solution as follows:

$$q[n]=q[0]-\frac{2\mathrm{i}|\Omega_1|}{|\Omega_2|}, \tag{3}$$

with the following matrix expression:

$$\Omega_2=\begin{pmatrix}
\lambda_1^{2n-2}\psi_1 & \lambda_1^{2n-4}\psi_1 & \cdots & \psi_1 & \lambda_1^{2n-1}\phi_1 & \lambda_1^{2n-3}\phi_1 & \cdots & \lambda_1\phi_1\\
\lambda_2^{2n-2}\psi_2 & \lambda_2^{2n-4}\psi_2 & \cdots & \psi_2 & \lambda_2^{2n-1}\phi_2 & \lambda_2^{2n-3}\phi_2 & \cdots & \lambda_2\phi_2\\
\vdots & \vdots & \cdots & \vdots & \vdots & \vdots & \cdots & \vdots\\
\lambda_n^{2n-2}\psi_n & \lambda_n^{2n-4}\psi_n & \cdots & \psi_n & \lambda_n^{2n-1}\phi_n & \lambda_n^{2n-3}\phi_n & \cdots & \lambda_n\phi_n\\
\lambda_1^{*2n-2}\phi_1^* & \lambda_1^{*2n-4}\phi_1^* & \cdots & \phi_1^* & -\lambda_1^{*2n-1}\psi_1^* & -\lambda_1^{*2n-3}\psi_1^* & \cdots & -\lambda_1^*\psi_1^*\\
\vdots & \vdots & \cdots & \vdots & \vdots & \vdots & \cdots & \vdots\\
\lambda_n^{*2n-2}\phi_n^* & \lambda_n^{*2n-4}\phi_n^* & \cdots & \phi_n^* & -\lambda_n^{*2n-1}\psi_n^* & -\lambda_n^{*2n-3}\psi_n^* & \cdots & -\lambda_n^*\psi_n^*
\end{pmatrix},$$

and Ω_1 is given by replacing the $(n+1)$-th column in Ω_2 with

$$(-\lambda_1^{2n}\psi_1,-\lambda_2^{2n}\psi_2,\ldots,-\lambda_n^{2n}\psi_n,-\lambda_1^{*2n}\phi_1^*,\ldots,-\lambda^{*2n}\phi_n^*)^{\mathrm{T}},$$

where $*$ denotes the complex conjugate and c_1,c_2 are the real coefficients,

$$\begin{aligned}
&\psi_j=[c_1(d\lambda_j\mathrm{e}^{B_j}+(H_j-D_j)\mathrm{e}^{-B_j})+c_2(-d\lambda_j\mathrm{e}^{-B_j}+(H_j+D_j)\mathrm{e}^{B_j})]\mathrm{e}^{A},\\
&\phi_j=[c_1((H_j-D_j)\mathrm{e}^{B_j}+d\lambda_j\mathrm{e}^{-B_j})+c_2((H_j+D_j)\mathrm{e}^{-B_j}-d\lambda_j\mathrm{e}^{B_j})]\mathrm{e}^{-A},\\
&A=\mathrm{i}(ax+bt),\qquad D_j=2\mathrm{i}\delta d^2+\mathrm{i}\lambda_j^2-\mathrm{i}a,\\
&H_j=\sqrt{-\left[\lambda_j^2+(2\delta d^2+\frac{1}{2}d^2-a)\right]^2-d^2\left(a-2\delta d^2-\frac{1}{4}d^2\right)},\\
&B=\frac{H_jx}{2}+H_jt\left\{\left(4\delta^2+3\delta+\frac{3}{8}\right)d^4+a^2+\left(\lambda_j^2+2\delta\right)a+\left(\lambda_j^2+\delta\right)^2+\left[\left(-4\delta-\frac{3}{2}\right)a-4\left(\frac{\lambda_j^2}{2}+\delta\right)\left(\delta+\frac{1}{4}\right)\right]d^2\right\},
\end{aligned}$$

Subsequently, we firstly consider the first-order solution, namely $n=1$. Assuming $H_1=H_{1,\mathrm{R}}+\mathrm{i}H_{1,\mathrm{I}}$, which corresponds to the spectral parameter $\lambda_1=\alpha_1+\mathrm{i}\beta_1$, we can find that the first-order solution comprises the hyperbolic function parts $\cosh(tV_{1,\mathrm{H}}+xH_{1,\mathrm{R}})$, $\sinh(tV_{1,\mathrm{H}}+xH_{1,\mathrm{R}})$ and the trigonometric function parts $\cos(tV_{1,\mathrm{T}}+xH_{1,\mathrm{I}})$, $\sin(tV_{1,\mathrm{T}}+xH_{1,\mathrm{I}})$, where the symbols R and I denote the real part and the imaginary part and

$$\begin{aligned}
&V_{1,\mathrm{H}}=W_1H_{1,\mathrm{R}}-W_2H_{1,\mathrm{I}},\ \ V_{1,\mathrm{T}}=W_1H_{1,\mathrm{I}}+W_2H_{1,\mathrm{R}},\ \ W_2=4\alpha_1\beta_1\Big(-2d^2\delta+2\delta-\frac{d^2}{2}-2\beta_1^2+2\alpha_1^2+a\Big),\\
&W_1=\frac{1}{4}\Bigg[32\left(d^2-\frac{1}{2}\right)^2\delta^2+\Big(24d^4-16\alpha_1^2d^2+16\beta_1^2d^2-32ad^2-8d^2-16\beta_1^2+16\alpha_1^2+16a\Big)\delta+3d^4\\
&\quad+\left(-4\alpha_1^2+4\beta_1^2-12a\right)d^2+8\alpha_1^4+\left(-48\beta_1^2+8a\right)\alpha_1^2+8\beta_1^4-8a\beta_1^2+8a^2\Bigg].
\end{aligned}$$

The above two function parts respectively describe the localization and periodicity of the wave's transverse distribution. In other words, the first-order solution is composed of the soliton parts and the periodic parts. It is obvious that the velocities of the two parts are $V_{1,\mathrm{H}}/H_{1,\mathrm{R}}$ and $V_{1,\mathrm{T}}/H_{1,\mathrm{I}}$, respectively. We can derive the first-order breather solution from Eq. (3) when $V_{1,\mathrm{H}}/H_{1,\mathrm{R}}\neq V_{1,\mathrm{T}}/H_{1,\mathrm{I}}$ holds. If $V_{1,\mathrm{H}}/H_{1,\mathrm{R}}=V_{1,\mathrm{T}}/H_{1,\mathrm{I}}$, the first-order solution will be converted into a continuous soliton. The breather-to-soliton state transition will be discussed.

2.1. The case $V_{1,\mathrm{H}}/H_{1,\mathrm{R}}\neq V_{1,\mathrm{T}}/H_{1,\mathrm{I}}$

In this case, the first-order solution becomes the localized wave solution with breathing behavior. By substitute $\lambda_1=\alpha_1+\mathrm{i}\beta_1$ into H_1, we obtain

$$H_1=\sqrt{-\left[\left(\alpha_1^2-\beta_1^2+\frac{1}{2}(4\delta+1)d^2-2a\right)+2\mathrm{i}\alpha\beta\right]^2+\frac{1}{4}d^4+d^2\left(2d^2\delta-a\right)}.$$

The condition $\alpha_1^2-\beta_1^2+(1/2)(4\delta+1)d^2-2a=0$ means the quantity under the square root is purely real, with no imaginary component, we call it condition I. When adding the following condition

$$4\beta_1^2\alpha_1^2+\frac{d^4}{4}+d^2\left(2d^2\delta-a\right)>0, \tag{4}$$

it means $H_{1,\mathrm{R}} \neq 0, H_{1,\mathrm{I}} = 0$, the general breather solution is obtained. The Akhmediev breather solution which is localized in time and periodic in space is presented when $H_{1,\mathrm{R}} = 0, H_{1,\mathrm{I}} \neq 0$, in other words, adding the condition

$$4\beta_1^2\alpha_1^2 + \frac{d^4}{4} + d^2\left(2d^2\delta - a\right) < 0. \tag{5}$$

2.2. The case $V_{1,\mathrm{H}}/H_{1,\mathrm{R}} = V_{1,\mathrm{T}}/H_{1,\mathrm{I}}$

In this case, the breather solution will be converted to the continuous soliton solution. We will discuss different types of the nonlinear converted waves. The condition $V_{1,\mathrm{H}}/H_{1,\mathrm{R}} = V_{1,\mathrm{T}}/H_{1,\mathrm{I}}$ can be expanded in the following form,

$$-2d^2\delta + 2\delta - \frac{1}{2}d^2 - 2\beta_1^2 + 2\alpha_1^2 + a = 0. \tag{6}$$

Given that the condition equation (6) is satisfied, we can obtain the multi-peak soliton as is shown in Fig. 1 by choosing appropriate parameters when the condition

$$\alpha_1^2 - \beta_1^2 + (1/2)(4\delta + 1)d^2 - 2a \neq 0$$

holds and we call it condition II. We can find that figures 1(a)–1(d) are the oscillation W-shaped soliton, while figures 1(e)–1(h) are the oscillation M-shaped soliton. Reversing the sign of the imaginary part β_1 of the eigenvalue leads to the transition between these two solitons. The waveform of each multi-peak soliton solution in Fig. 1 maintains its stability without change across different time points. Furthermore, when the parameters a, b, d, δ are given, the condition (6) can be written as $2\alpha_1^2 - 2\beta_1^2 - 1/10 = 0$. Then the real part α_1 of the parameter λ_1 satisfies $\alpha_1 > \sqrt{5}/10$. It is observed that when $\sqrt{5}/10 < \alpha_1 < 1$ and keeps decreasing, the number of wave peaks for the oscillation W-shaped and M-shaped soliton will increase.

Based on the condition (6), we add condition I. In this case, the periodic wave solution and anti-dark soliton solution are obtained. We can derive two different types of periodic wave solutions as shown in Fig. 2 by selecting appropriate parameters when the condition equation (5) is satisfied.

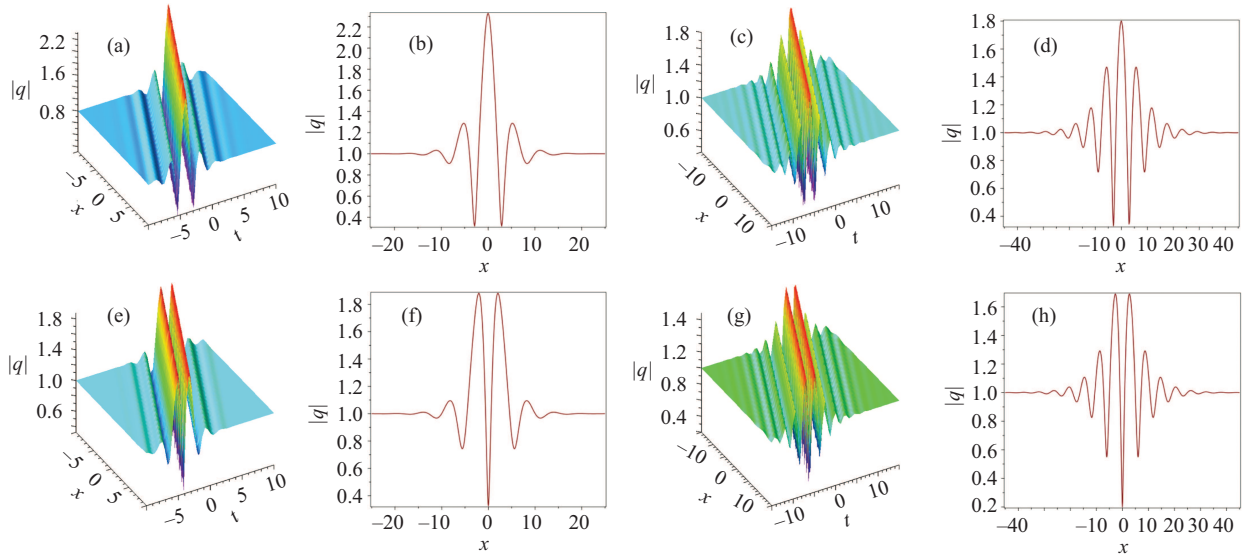


Fig. 1. The multi-peak soliton solution with $a = 2/5$, $d = 1$, $\delta = 7/10$, $c_1 = c_2 = 2$, $b = -5.109$. (a) The oscillation W-shaped soliton with $\lambda_1 = 2/5 - (\sqrt{11}/10)\mathrm{i}$, (b) the cross-sectional view of (a) at $t = 0$, (c) the oscillation W-shaped soliton with $\lambda_1 = 3/10 - (1/5)\mathrm{i}$, (d) the cross-sectional view of (c) at $t = 0$, (e) the oscillation M-shaped soliton with $\lambda_1 = 2/5 + (\sqrt{11}/10)\mathrm{i}$, (f) the cross-sectional view of (e) at $t = 0$, (g) the oscillation M-shaped soliton with $\lambda_1 = 3/10 + (1/5)\mathrm{i}$, (h) the cross-sectional view of (g) at $t = 0$.

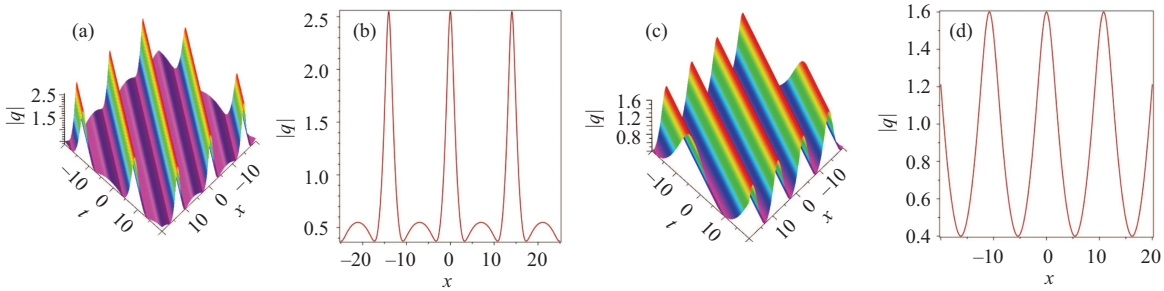


Fig. 2. The periodic wave solution with $a = 3/10$, $d = 1$, $\delta = -3/20$, $c_1 = c_2 = 2$, $b = -1/160$. (a) $\lambda = 1/2 + (\sqrt{15}/10)\mathrm{i}$, (b) the cross-sectional view of (a) at $t = 0$, (c) $\lambda = 7/20 + (3/20)\mathrm{i}$, (d) the cross-sectional view of (d) at $t = 0$.

It is worth noting that the period of the periodic wave is $2\pi/H_{\mathrm{I}}$, hence when the period extends to infinity, namely $H_{\mathrm{I}} \to 0$, the periodic wave solution will be converted to the W-shaped soliton solution as is presented in Figs. 3(a) and 3(b). The W-shaped soliton solution is rational without the hyperbolic function and the trigonometric function, we show its explicit expression

as follows:

$$q_{rs}=\frac{-213000\left[-\frac{639}{1000}t^2+\left(\mathrm{i}+\frac{6}{5}x\right)t-\frac{200\mathrm{i}}{213}x-\frac{40}{71}x^2+\frac{200}{71}\right]\exp\left[-\frac{\mathrm{i}}{160}(t-48x)\right]}{-136107t^2+(213000\mathrm{i}+255600x)t-200000\mathrm{i}x-120000x^2-200000}.$$

Subsequently, when the condition (4) holds, the first-order solution can be degenerate into the anti-dark soliton solution which is a bell-shaped localized wave on the plane wave background in Figs. 3(c) and 3(d).

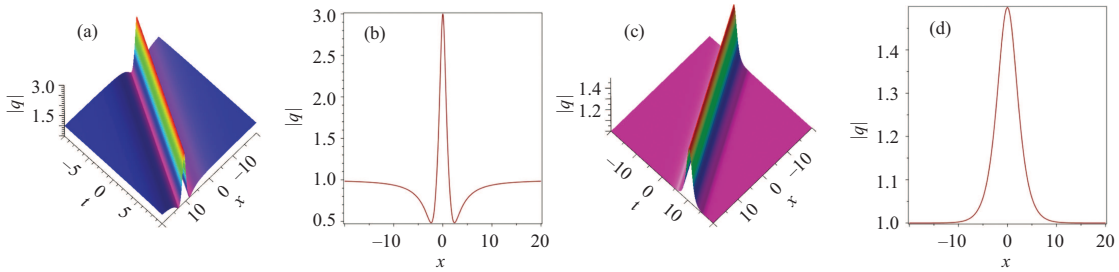


Fig. 3. (a) The W-shaped soliton degenerated from the periodic wave Fig. 2(a) with $\lambda_1=\sqrt{35}/10-(1/2)\mathrm{i}$, $a=3/10$, $d=1$, $\delta=-3/50$, $c_1=c_2=1$, $b=-1/160$; (b) The cross-sectional view of (a) at $t=0$; (c) The anti-dark soliton with $\lambda_1=7/10+(\sqrt{59}/10)\mathrm{i}$, $a=3/10$, $d=1$, $\delta=-3/20$, $c_1=c_2=2$, $b=-1/160$; (d) The cross-sectional view of (c) at $t=0$.

3. Nonlinear wave interactions

In this section, the breather-to-soliton state transition of the second-order solution is discussed. When $n=2$, we have $H_2=H_{2,\mathrm{R}}+\mathrm{i}H_{2,\mathrm{I}}$ which corresponds to the spectral parameter $\lambda_2=\alpha_2+\mathrm{i}\beta_2$. Then the second-order solution contains an additional hyperbolic function part $\cosh(V_{2,\mathrm{H}}t+H_{2,\mathrm{R}}x)$, $\sinh(V_{2,\mathrm{H}}t+H_{2,\mathrm{R}}x)$ and a trigonometric function part $\cos(V_{2,\mathrm{T}}t+H_{2,\mathrm{I}}x)$, $\sin(V_{2,\mathrm{T}}t+H_{2,\mathrm{I}}x)$ compared to the first-order solution. Thus, due to the existence of two eigenvalue parameters, except for the condition of the case 2.1 or the case 2.2, it is necessary to take into account another condition, namely $V_{2,\mathrm{H}}/H_{2,\mathrm{R}}=V_{2,\mathrm{T}}/H_{2,\mathrm{I}}$ or $V_{2,\mathrm{H}}/H_{2,\mathrm{R}}\neq V_{2,\mathrm{T}}/H_{2,\mathrm{I}}$.

Firstly, under the conditions $V_{1,\mathrm{H}}/H_{1,\mathrm{R}}=V_{1,\mathrm{T}}/H_{1,\mathrm{I}}$ and $V_{2,\mathrm{H}}/H_{2,\mathrm{R}}\neq V_{2,\mathrm{T}}/H_{2,\mathrm{I}}$, the interactions between the breather and other nonlinear converted waves can be obtained under $c_1=c_2=2$. Figure 4(a) exhibits the interaction between the breather and the anti-dark soliton when additional condition I and condition (4) are satisfied. When the condition (5) holds, we can obtain the interaction between the breather and the periodic wave as is shown in Fig. 4(b). Moreover, under Condition I, the second-order solution is degenerated into the interaction between the breather and multi-peak soliton and we can see Fig. 4(c).

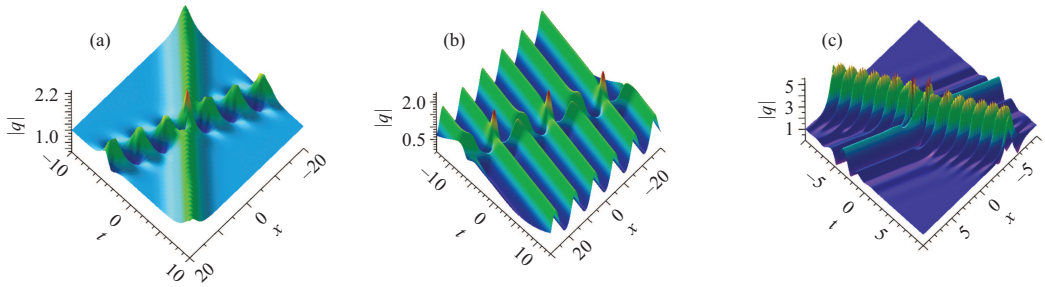


Fig. 4. The interaction solutions: (a) the breather and the anti-dark soliton with $\lambda_1=7/10+(\sqrt{59}/10)\mathrm{i}$, $\lambda_2=1+(1/5)\mathrm{i}$, $a=3/10$, $d=1$, $\delta=-3/20$, $b=-1/160$; (b) the breather and the periodic wave with $\lambda_1=7/20-(3/20)\mathrm{i}$, $\lambda_2=1-(1/5)\mathrm{i}$, $a=3/10$, $d=1$, $\delta=-3/20$, $b=-1/160$; (c) the breather and the multi-peak soliton with $\lambda_1=2/5-(\sqrt{11}/10)\mathrm{i}$, $\lambda_2=-1/2+\mathrm{i}$, $a=2/5$, $d=1$, $\delta=7/10$, $b=-5.109$.

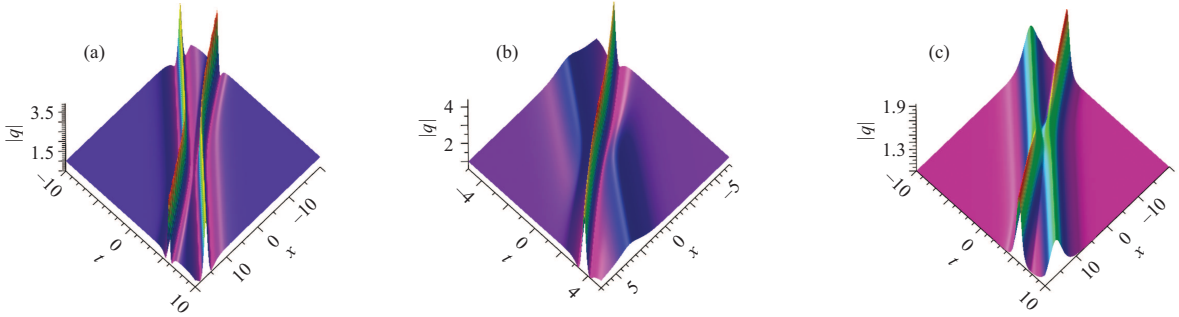


Fig. 5. The interaction solutions when $a=3/10$, $d=1$, $\delta=-3/20$, $b=-1/160$. (a) The W-shaped soliton and the W-shaped soliton with $\lambda_1=7/10-(\sqrt{39}/10)\mathrm{i}$, $\lambda_2=-4/5+(3\sqrt{6}/10)\mathrm{i}$; (b) the anti-dark soliton and the W-shaped soliton with $\lambda_1=7/10+(\sqrt{39}/10)\mathrm{i}$, $\lambda_2=-4/5+(3\sqrt{6}/10)\mathrm{i}$; (c) the anti-dark soliton and the anti-dark soliton with $\lambda_1=7/10+(\sqrt{39}/10)\mathrm{i}$, $\lambda_2=4/5-(3\sqrt{6}/10)\mathrm{i}$.

Subsequently, based on the conditions $V_{1,\mathrm{H}}/H_{1,\mathrm{R}} = V_{1,\mathrm{T}}/H_{1,\mathrm{I}}$ and $V_{2,\mathrm{H}}/H_{2,\mathrm{R}} = V_{2,\mathrm{T}}/H_{2,\mathrm{I}}$, when the conditions $\alpha_j^2 - \beta_j^2 + [(4\delta+1)d^2 - 2a]/2 = 0$, $j = 1,2$ hold and $4\beta_j^2\alpha_j^2 + d^4/4 + d^2\left(2d^2\delta - a\right)$, $j = 1,2$ have the same signs, we obtain the interaction about the W-shaped soliton and the anti-dark soliton under $c_1 = c_2 = 2$. In Fig. 5(a), the interaction between the W-shaped solitons is obtained. The interaction between the W-shaped soliton and the anti-dark soliton is presented in Fig. 5(b). Meanwhile, we can also derive the interaction between the anti-dark solitons in Fig. 5(c).

4. Double-pole breather-to-soliton transitions

In this section, we start with the double-pole solution of Eq. (1) given in Ref. [35] to investigate the double-pole breather-to-soliton transitions. It is known that the double-pole solution can be rewritten as

$$q[2] = q[0] - \frac{2\mathrm{i}|\Omega_3|}{|\Omega_4|}, \tag{7}$$

with

$$\Omega_4 = \left(S_1, \frac{d}{d\varepsilon}S_1, S_2, \frac{d}{d\varepsilon}S_2\right)^{\mathrm{T}},$$

$$\Omega_3 = \left(S_3, \frac{d}{d\varepsilon}S_3, S_4, \frac{d}{d\varepsilon}S_4\right)^{\mathrm{T}},$$

$$S_1 = \lim_{\varepsilon\to 0}\left[\left(\lambda_1^2\psi_1, \psi_1, -\lambda_1^4\psi_1, \lambda_1\phi_1\right)^{\mathrm{T}}|_{\lambda_1=\lambda_1+\varepsilon}\right],$$

$$S_2 = \lim_{\varepsilon\to 0}\left[\left(\lambda_1^{*2}\phi_{1,*}, \phi_1^*, -\lambda_1^{*4}\phi_1^*, -\lambda_1^*\psi_1^*\right)^{\mathrm{T}}|_{\lambda_1=\lambda_1+\varepsilon}\right],$$

$$S_3 = \lim_{\varepsilon\to 0}\left[\left(\lambda_1^2\psi_1, \psi_1, -\lambda_1^3\phi_1, \lambda_1\phi_1\right)^{\mathrm{T}}|_{\lambda_1=\lambda_1+\varepsilon}\right],$$

$$S_4 = \lim_{\varepsilon\to 0}\left[\left(\lambda_1^{*2}\phi_{1,*}, \phi_1^*, -\lambda_1^{*3}\psi_1^*, -\lambda_1^*\psi_1^*\right)^{\mathrm{T}}|_{\lambda_1=\lambda_1+\varepsilon}\right],$$

where ε is a small parameter and ϕ_1, ψ_1 are the same as in Eq. (3).

Similarly, the state transition condition of the double-pole solution is $V_{1,\mathrm{H}}/H_{1,\mathrm{R}} = V_{1,\mathrm{T}}/H_{1,\mathrm{I}}$. Based on the condition, we will obtain multiple double-pole converted wave solutions. When the additional condition II is satisfied, the double-pole solution can be reduced into the double-pole multi-peak soliton solution. We can see that figure 6(a) presents the interaction between two series of the double-pole multi-peak soliton. Their wave peaks achieve the maximal amplitude at $(0,0)$. If condition I holds, when equations (4) and (5) are satisfied respectively, we can obtain the double-pole periodic wave solution and the double-pole anti-dark soliton solution as is shown in Figs. 6(b) and 6(c), respectively. The former possesses a periodic chained higher-amplitude region which exhibits double-pole phenomena.

We will apply the asymptotic analysis method described in Ref. [36] to explore the asymptotic behavior of the double-pole anti-dark soliton. For convenience, assuming $d = 1$, $c_1 = c_2 = 2$, $\lambda_1 = \alpha_1 + \mathrm{i}\beta_1$ under the corresponding state transition conditions, we can obtain $a = \alpha_1^2 - \beta_1^2 + (4\delta+1)/2$, $\delta = -3\alpha_1^2/2 + 3\beta_1^2/2$, and $4\beta_1^2 > 1$. Hence, the double-pole anti-dark soliton solution is

$$q_d = \frac{3072\,\mathrm{e}^{\mathrm{i}D_1}\left(E_1\,\mathrm{e}^{(D_2\Delta)/8} + E_2\,\mathrm{e}^{3(D_2\Delta)/8} + E_3\,\mathrm{e}^{(D_2\Delta)/2} - 1/2E_4\,\mathrm{e}^{(D_2\Delta)/4} - E_5\right)}{G_1\,\mathrm{e}^{(D_2\Delta)/2} + G_2\,\mathrm{e}^{(D_2\Delta)/4} + 384\beta(G_3\,\mathrm{e}^{(D_2\Delta)/8} + G_4\,\mathrm{e}^{3(D_2\Delta)/8} - G_5)}, \tag{8}$$

where

$$D_1 = \frac{25(\beta_1-\alpha_1)^3(\beta_1+\alpha_1)^3 t}{4} + 2\left(\beta_1^2 - \alpha_1^2 + \frac{1}{4}\right)x,$$

$$D_2 = \left(6\beta_1^4 + 4(5\alpha_1^2-1)\beta_1^2 + 6\alpha_1^4 + 4\alpha_1^2 + 1\right)t - 4x, \quad \Delta = \sqrt{(4\beta_1^2-1)(4\alpha_1^2+1)},$$

and E_j, $j = 1,\ldots,5$ and G_j, $j = 1,\ldots,5$ are too long to be included here, so we omit them.

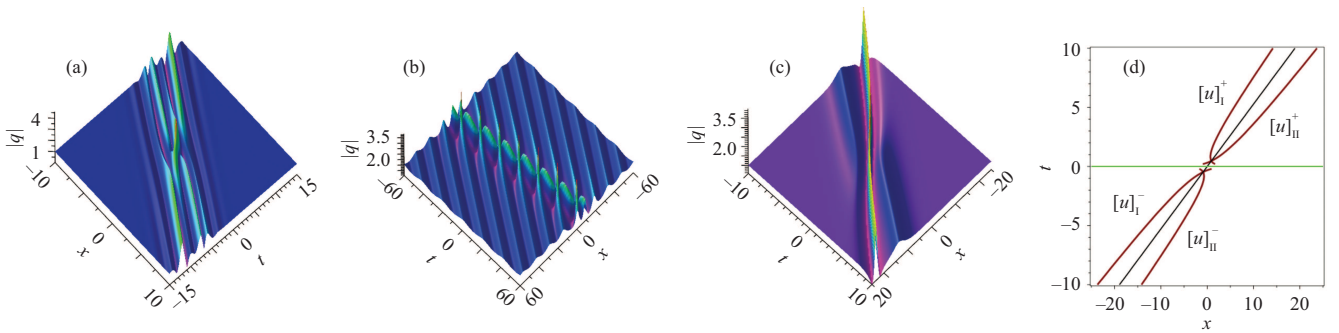


Fig. 6. (a) The double-pole multi-peak soliton solution with $\lambda_1 = 1/2 - (\sqrt{5}/5)\mathrm{i}$, $a = 2/5$, $d = 1$, $\delta = 7/10$, $b = -5.109$; (b) The double-pole periodic wave solution with $\lambda_1 = 1/2 - (\sqrt{15}/5)\mathrm{i}$, $a = 3/10$, $d = 1$, $\delta = -3/20$, $b = -1/160$; (c) The double-pole anti-dark soliton with $\lambda_1 = 7/10 + (\sqrt{39}/10)\mathrm{i}$, $a = 3/10$, $d = 1$, $\delta = -3/20$, $b = -1/160$; (d) The wave crest line graph (red line) for the asymptotic solitons of (c) with $\alpha_1 = 7/10$, $\beta_1 = \sqrt{39}/10$. Auxiliary lines: Green: $t = 0$; Black: $4x - 7.5752t = 0$.

Subsequently, we substitute $x=\left[\left(6\beta_1^4+4(5\alpha_1^2-1)\beta_1^2+6\alpha_1^4+4\alpha_1^2+1\right)t-D_2\right]/4$ into Eq. (8) so that the expression of the double-pole solution is only related to D_2 and t. Numerous articles about the asymptotic analysis method have illustrated that the characteristic line of the double-pole solution is curved.[36–38] Therefore, if we want to derive the asymptotic soliton, an asymptotic balance relation between $\mathrm{e}^{\pm D_2}$ and t need to be satisfied.[39] The explicit expressions of the asymptotic solitons in general form are exhibited below.

(i) When $\mathrm{e}^{D_2}\sim t$,

$$[u]_{\mathrm{I}}^{\pm}\to \mathrm{e}^{D_1}\left[1+\frac{K_1}{2K_2\cosh\left((D_2\Delta)/8+\ln K_3\right)+384\beta_1K_4}\right],\qquad t\to\pm\infty, \tag{9}$$

where

$$\begin{aligned}
&K_1=32(2\beta_1+1)^2(2\beta_1-1)^2(4\alpha_1^2+1)^2(\alpha_1^2+\beta_1^2)\beta_1^3\left(4\mathrm{i}\beta_1^2-\mathrm{i}-\Delta\right)t,\\
&K_2=32\sqrt{2}\sqrt{-\beta_1^8\left(\Delta\mathrm{i}+2\beta_1^2-2\alpha_1^2-1\right)(\alpha_1^2+\beta_1^2)^3\Delta^3|t|},\\
&K_3=\frac{\sqrt{2}\beta_1^4\sqrt{\Delta\mathrm{i}+2\beta_1^2-2\alpha_1^2-1}(\alpha_1^2+\beta_1^2)}{2\sqrt{-\beta_1^8(\alpha_1^2+\beta_1^2)^3\Delta^3|t|}},\qquad K_4=\frac{1}{24}\Delta^2(4\alpha_1^2+1)(\alpha_1^2+\beta_1^2)\beta_1^2\left(4\mathrm{i}\beta_1^2-\mathrm{i}-\Delta\right)t.
\end{aligned}$$

(ii) When $\mathrm{e}^{-D_2}\sim t$,

$$[u]_{\mathrm{II}}^{\pm}\to \mathrm{e}^{D_1}\left[1+\frac{L_1}{2L_2\cosh\left((D_2\Delta)/8+\ln L_3\right)+384\beta_1L_4}\right],\qquad t\to\pm\infty, \tag{10}$$

where

$$\begin{aligned}
&L_1=32(2\beta_1+1)^2(2\beta_1-1)^2(4\alpha_1^2+1)^2(\alpha_1^2+\beta_1^2)\beta_1^3\left(4\mathrm{i}\beta_1^2-\mathrm{i}+\Delta\right)t,\\
&L_2=32\sqrt{2}\sqrt{\beta_1^8\left(\Delta\mathrm{i}-2\beta_1^2+2\alpha_1^2+1\right)(\alpha_1^2+\beta_1^2)^3\Delta^3|t|},\\
&L_3=-\frac{\sqrt{2}\beta_1^4\Delta^3\sqrt{\alpha_1^2+\beta_1^2}|t|}{\sqrt{\beta_1^8(\Delta\mathrm{i}-2\beta_1^2+2\alpha_1^2+1)}},\qquad L_4=\frac{1}{24}\Delta^2(4\alpha_1^2+1)(\alpha_1^2+\beta_1^2)\beta_1^2\left(4\mathrm{i}\beta_1^2-\mathrm{i}+\Delta\right)t.
\end{aligned}$$

We can find the characteristic lines of the asymptotic solitons above are $(D_2\Delta)/8+\ln K_3=0$ and $D_2\Delta/8+\ln L_3=0$, both contain the logarithmic terms which can reflect the double-pole properties. When $a=3/10$, $d=1$, $\delta=-3/20$, $\lambda_1=7/10+(\sqrt{39}/10)\mathrm{i}$ are taken, it can be observed that the wave crest line graph of the corresponding asymptotic solitons in Fig. 6(d) is associated with the contour plot in Fig. 6(c). Furthermore, we compare the asymptotic solitons (9), (10) with the exact solution (3) under specific parameter settings. As is evident in Fig. 7, the asymptotic solitons match the exact solution perfectly in the far-field region, which further validates the reliability of our asymptotic analysis.

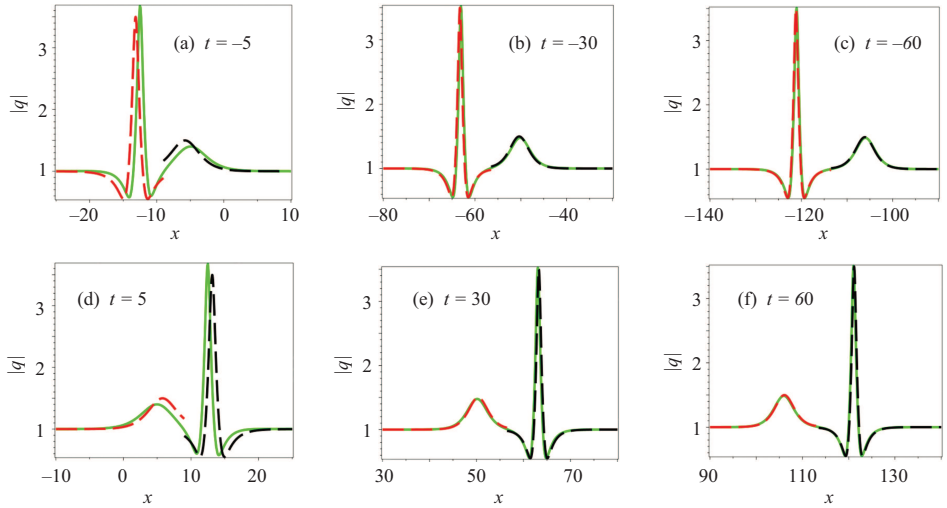


Fig. 7. The comparisons of the asymptotic solitons and the exact solution (green line) for the double-pole anti-dark soliton in Fig. 6(c). (a)–(c) red: the asymptotic soliton $[u]_{\mathrm{I}}^{-}$, black: the asymptotic soliton $[u]_{\mathrm{II}}^{-}$; (d)–(f) red: the asymptotic soliton $[u]_{\mathrm{I}}^{+}$, black: the asymptotic soliton $[u]_{\mathrm{II}}^{+}$.

5. Conclusions

In conclusion, we explored the breather-to-soliton transitions and nonlinear wave interactions for the HGGI equation. The following key conclusions have been drawn.

A rich family of the breather-to-soliton nonlinear converted waves are obtained. Notably, these structures exhibit distinct dynamical features which have not been reported in lower-order GI models. The elastic interactions between various nonlinear converted waves were exhibited. These interactions are characterized by the fact that the amplitude, velocity, and shape of the localized waves remain unchanged both before and after collision. The double-pole breather-to-soliton transitions were studied. Asymptotic analysis shows double-pole anti-dark solitons evolve into stable structures over long propagation, due to the interplay of self-steepening and Raman terms in the HGGI equation.

Our work enriches the localized wave structures and the related dynamical properties for the HGGI equation. It will provide a reference for future projects about the breather-to-soliton transitions for the higher-order nonlinear evolution equations.

Acknowledgments

The authors thanks Prof. Q. P. Liu for helpful and enlightening suggestions. Project supported by the Fundamental Research Funds for the Central Universities (Grant No. 3072025CFJ2405).

References

[1] Vinayagam P S, Radha R and Porsezian K 2013 *Phys. Rev. E* **88** 042906
[2] Saha A, Pradhan B and Banerjee S 2020 *Phys. Scr.* **95** 055602
[3] Copi F, Randoux S and Suret P 2020 *Rev. Phys.* **5** 100037
[4] Rizvi S and Shabbir S 2023 *Optik* **294** 171456
[5] Mao Y F, Chandramouli S, Xu W Q and Hoefer A M 2023 *Phys. Rev. Lett.* **131** 147201
[6] Rizvi S and Mustafa B 2024 *Opt. Quantum Electron.* **56** 393
[7] Mahnke C and Mitschke F 2012 *Phys. Rev. E* **85** 033808
[8] Yang G Y, Wang Y, Qin Z Y, Malomed B A, Mihalache D and Li L 2014 *Phys. Rev. E* **90** 062909
[9] Liu C F, Hu K, Hu T and Tang Y 2011 *Chin. Phys. B* **20** 010309
[10] Liu C F, Lu M and Liu W Q 2012 *Phys. Lett. A* **376** 188
[11] Zheng L, Zhang Y C and Liu C F 2019 *Chin. Phys. B* **28** 116701
[12] Liu C, Yang Z Y, Zhao L C and Yang W L 2015 *Phys. Rev. E* **91** 022904
[13] He J S, Xu S W, Ruderman M S and Erdélyi R 2014 *Chin. Phys. Lett.* **31** 010502
[14] Chowdury A, Kedziora D J, Ankiewicz A and Akhmediev N 2015 *Phys. Rev. E* **91** 032928
[15] Wang L, Zhang J H, Wang Z Q, Liu C, Li M, Qi F H and Guo R 2016 *Phys. Rev. E* **93** 012214
[16] Huang Q M, Gao Y T and Hu L 2018 *Appl. Math. Lett.* **75** 135
[17] Chowdury A, Ankiewicz A and Akhmediev N 2015 *Proc. R. Soc. A* **471** 20150130
[18] Wang L, Zhang J H, Liu C, Li M and Qi F H 2016 *Phys. Rev. E* **93** 062217
[19] Wu X H, Gao Y T and Yu X 2014 *Chaos, Solitons and Fractals* **183** 114874
[20] Zhao L C, Li S C and Ling L M 2016 *Phys. Rev. E* **93** 032215
[21] Niu J X, Guo R and Zhang J W 2023 *Wave Motion* **123** 103233
[22] Wang J N, Liu M W, Zhang Z Y, Wang H T and Liu W J 2024 *Phys. Rev. E* **524** 129823
[23] Wang L, Zhu Y J, Wang Z Q, Xu T, Qi F H and Xue Y S 2016 *J. Phys. Soc. Jpn.* **85** 024001
[24] Liu C, Yang Z Y, Zhao L C and Yang W L 2015 *Ann. Phys.* **362** 130
[25] Wang L, Wang Z Q, Zhang J H, Qi F H and Li M 2016 *Nonlinear Dyn.* **86** 185
[26] Zhang H S, Wang L, Wang X and Xie X Y 2020 *Nonlinear Dyn.* **102** 349
[27] Zhang H S, Wang L, Sun W R, Wang X and Xu T 2021 *Physica D* **419** 132849
[28] Du Z, Meng G Q and Du X X 2021 *Chaos, Solitons and Fractals* **153** 111507
[29] Liu S H, Tian B and Gao X T 2024 *Eur. Phys. J. Plus* **139** 496
[30] Olmedilla E 1987 *Physica D* **25** 330
[31] Gagnon L and Stiévenart N 1994 *Opt. Lett.* **19** 619
[32] Li M, Xiao J H, Liu W J, Jiang Y, Sun K and Tian B 2011 *Phys. Lett. A* **375** 549
[33] Guan X, Yang H, Meng X and Liu W J 2023 *Appl. Math. Lett.* **136** 108466
[34] Zhao Y D, Wang Y F, Yang S X, Zhang X and Chen Y X 2024 *Chaos, Solitons and Fractals* **185** 115147
[35] Zhao Y D, Wang Y F, Zhang X and Chen Y X 2025 *Nonlinear Dyn.* **113** 15257
[36] Li M, Zhang X, Xu T and Li L L 2020 *J. Phys. Soc. Jpn.* **89** 054004
[37] Wu X H, Gao Y T and Yu X 2023 *Nonlinear Dyn.* **111** 14421
[38] Li P, He J S and Li M H 2024 *Nonlinear Dyn.* **112** 10239
[39] Li M, Yue X L and Xu T 2020 *Phys. Scr.* **95** 055222